International Journal of Fracture **117:** 113–128, 2002.

Analytical solutions for two penny-shaped crack problems in thermo-piezoelectric materials and their finite element comparisons

FULIN SHANG, MEINHARD KUNA* and MATTHIAS SCHERZER
Freiberg University of Mining and Technology, Institute of Mechanics and Fluid Dynamics, Lampadiustrasse 4, D-09596 Freiberg, Germany; (Corresponding author (Tel: +49 (03731) 392092; Fax: +49 (03731) 393455; e-mail: meinhard.kuna@imfd.tu-freiberg.de)

Received 28 August 2001; accepted in revised form 3 July 2002

Abstract. Thermally loaded penny-shaped cracks in thermopiezoelectric materials are investigated in this paper. The analytical solutions for the penny-shaped cracks subjected to uniform temperature and steady heat flow are discussed. Comparisons are made between the stress-intensity factors derived by the analytical solutions and the numerical results using different finite element techniques.

Key words: Penny-shaped crack, thermopiezoelectric material, analytical solution, finite element method.

1. Introduction

With the introduction of fracture mechanics concept into piezoelectric materials, many crack problems in piezoelectric solids have been addressed analytically, see for example Sosa and Pak (1990), Sosa (1991), Pak (1992), Suo et al. (1992), Wang (1992), Wang (1994), Wang and Huang (1995), Chen and Shioya (1999). Meanwhile, various finite element techniques have been established for electromechanical crack analyses by Kuna (1998), and their efficiency has been demonstrated for a variety of three-dimensional (3D) crack problems by Shang et al. (2001). These theoretical-numerical developments are indispensable to assess strength and reliability of piezoelectric structures containing crack-like defects.

Following this, research progresses on crack problems in thermopiezoelectric materials were reported during last decade. A two-dimensional analytical solution for a finite crack in thermopiezoelectric solids was presented by Yu and Qin (1996) using Fourier transform and extended Stroh formalism. Analyzed in Qin (1998) is a problem of insulated elliptical hole embedded in an infinite thermopiezoelectric plate. One of the present authors proposed a general solution based on potential functions for 3D axisymmetric problems in thermo-piezoelectric materials, and the exact solutions for penny-shaped cracks under thermal excitation were obtained in (Shang et al., 1996a, b, c) by means of Hankel transform. Numerical tools are needed to analyze crack-like defects in thermopiezoelectric structures as well. More recently, several finite element techniques were developed to analyze the behavior of thermopiezoelectric materials (Shang et al., 2001b). Thus, it is possible to verify the analytical solutions obtained above numerically.

In what follows, the analytical solutions and numerical results will be presented for 3D cracks in thermopiezoelectric materials. The analytical solutions for penny-shaped cracks

subjected to different thermal loadings will be reviewed and discussed. The numerical results of stress intensity factor (SIF) will be compared with the analytical ones.

2. Potential function formulation

The general solution method of potential functions for 3D axisymmetric problems in transversely isotropic thermopiezoelectric medium developed by the authors (Shang et al., 1996a) will be reviewed briefly in this section.

The constitutive relations for a thermopiezoelectric continuum are given by

$$\begin{aligned} \sigma_{ij} &= c_{ijkl}\varepsilon_{kl} - e_{kij}E_k - \lambda_{ij}\theta \\ D_i &= e_{ijk}\varepsilon_{jk} + \in_{ij} E_j + p_i\theta \\ \rho\eta &= \lambda_{ij}\varepsilon_{ij} + p_i E_i + \rho\theta\, C_v/\Theta, \end{aligned} \tag{1}$$

where c_{ijkl}, e_{kij}, λ_{ij}, $\in_{ij}$, p_i are the elastic constants, piezoelectric modules, temperature stress coefficients, dielectric constants, pyroelectric constants, respectively; C_v is the heat capacity per unit volume at constant strain; ρ is the mass density; σ_{ij}, ε_{ij}, D_i, E_i denote the stress, strain, electric displacement, and electric field, respectively; η is the specific entropy; Θ is the absolute temperature; $\theta = \Theta - \Theta_0$ is the temperature change from a stress free reference temperature Θ_0.

The governing equations for thermopiezoelectricity include three fundamental equations: (1) the equation of motion, (2) the equation of the quasi stationary electric field, and (3) the heat conduction equation. For a stationary case, the system of differential equations for the field variables u_i, φ and θ is given by

$$\begin{aligned} \sigma_{ij,j} &= c_{ijkl}u_{k,lj} + e_{kij}\varphi_{,kj} - \lambda_{ij}\theta_{,j} = 0 \\ D_{i,i} &= e_{ikl}u_{k,li} - \in_{ik} \varphi_{,ki} + p_i\theta_{,i} = 0 \\ \kappa_{ij}\theta_{,ij} &= 0, \end{aligned} \tag{2}$$

where κ_{ij} are the heat conduction coefficients.

The steady-state temperature field considered can be expressed conveniently in terms of the cylindrical coordinates (ρ, α, z)shown in Figure 1 as

$$\theta(\rho, z) = \int_0^\infty A(\zeta) J_0(\zeta\rho) e^{-\zeta z/\kappa} d\zeta, \tag{3}$$

where $J_n(x)$ is the Bessel function of the first kind and n-th order, $\kappa^2 = \kappa_{33}/\kappa_{11}$ is the ratio of heat conduction constants in the axial z-direction and in the radial ρ-direction, and $A(\zeta)$ is the unknown to be determined through thermal boundary conditions.

Four potential functions ψ, ψ_1, ψ_2, ψ_3 were introduced to solve the governing equations (Shang et al. 1996c). These functions can be written in the form as

$$\begin{aligned} u_\rho &= \frac{\partial}{\partial\rho}(\psi_1 + \psi_2 + \psi_3 + \psi) \\ u_z &= \frac{\partial}{\partial z}(l_{11}\psi_1 + l_{12}\psi_2 + l_{13}\psi_3 + l_{14}\psi) \\ \varphi &= \frac{\partial}{\partial z}(l_{21}\psi_1 + l_{22}\psi_2 + l_{23}\psi_3 + l_{24}\psi) \end{aligned} \tag{4a}$$

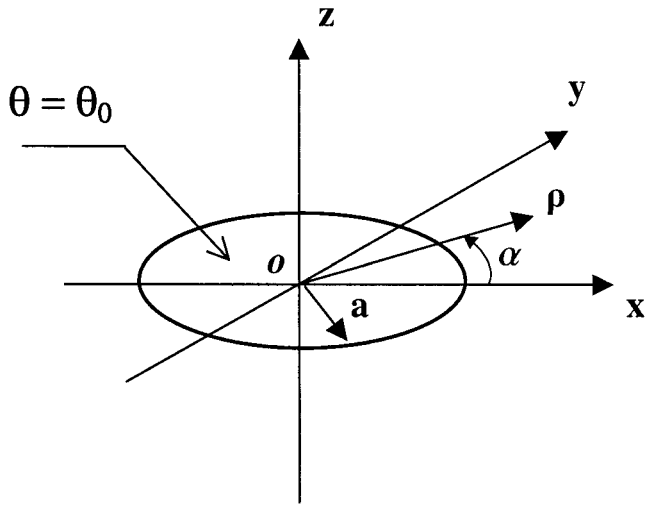

Figure 1. Penny-shaped crack with uniform temperature on its surface.

$$\psi_j(\rho, z) = \int_0^\infty F_j(\zeta) J_0(\zeta\rho) e^{-\zeta z/\gamma_j} d\zeta \qquad j = 1,\ 2,\ 3$$

$$\psi(\rho, z) = \int_0^\infty A(\zeta) C(\zeta) J_0(\zeta\rho) e^{-\zeta z/\kappa} d\zeta, \tag{4b}$$

where $F_j(\zeta)$ and $C(\zeta)$ are the functions to be determined through boundary conditions. The three eigenvalues γ_j can be determined by solving a cubic algebraic equation. The three roots of the derived cubic equation are either three real numbers or one real number and two conjugate complex numbers. Corresponding to these three roots, the potential functions ψ_j satisfy quasi-harmonic equations as

$$\frac{\partial^2 \psi_j}{\partial \rho^2} + \frac{1}{\rho}\frac{\partial \psi_j}{\partial \rho} + \gamma_j^2 \frac{\partial^2 \psi_j}{\partial z^2} = 0 \tag{5}$$

The eigenvalues γ_j are related to elastic, piezoelectric and dielectric material constants as

$$\frac{a_j + c_{13} l_{1j} + e_{31} l_{2j}}{c_{11}} = \frac{c_{33} l_{1j} + e_{33} l_{2j}}{c_{13} + a_j} = \frac{e_{33} l_{1j} - \in_{33} l_{2j}}{d_j + e_{31}} = \gamma_j^2, \quad j = 1, 2, 3, \tag{6}$$

where $a_i = c_{44}(1 + l_{1i}) + e_{15} l_{2i}$, $d_i = e_{15}(1 + l_{1i}) - \in_{11} l_{2i}$, $i = 1, 2, 3, 4$ and l_{1j}, l_{2j} are unknown constants. Through analyzing the above relations, we found that the six constants l_{1j}, l_{2j} can be uniquely given out from the six relations (6) corresponding to three eigenvalues γ_j. The lengthy expressions, which are not presented here, were given out with the aid of a symbolic manipulation software, *Mathematica* (see Shang et al., 2001a).

Further, $C(\zeta)$, l_{14}, l_{24} can be explicitly given out from the fourth eigenvalue κ as

$$\begin{aligned}
&\zeta^2 C(\zeta) = \lambda_{11}\kappa^2 \big/ (c_{44} + c_0 l_{14} + e_0 l_{24} - c_{11}\kappa^2) = m = const. \\
&l_{14} = (B_2 C_1 - B_1 C_2) \big/ (B_2 A_1 - B_1 A_2) \qquad l_{24} = (C_1 - l_{14} A_1) \big/ B_1 \\
&A_1 = c_{33} - \kappa^2 c_{44} - c_0 \lambda_{33} \big/ \lambda_{11} \qquad A_2 = e_{33} - \kappa^2 e_{15} + p_3 c_0 \big/ \lambda_{11} \\
&B_1 = e_{33} - \kappa^2 e_{15} - e_0 \lambda_{33} \big/ \lambda_{11} \qquad B_2 = - \in_{33} + \kappa^2 \in_{11} + p_3 e_0 \big/ \lambda_{11} \\
&C_1 = \kappa^2 c_0 + (c_{44} - c_{11}\kappa^2)\lambda_{33} \big/ \lambda_{11} \qquad C_2 = \kappa^2 e_0 - (c_{44} - c_{11}\kappa^2) p_3 \big/ \lambda_{11} \\
&c_0 = c_{13} + c_{44} \qquad e_0 = e_{31} + e_{15}
\end{aligned} \tag{7}$$

3. Analytical solutions of thermally loaded penny-shaped cracks

The analytical solutions of thermally loaded penny-shaped cracks, which were initially obtained in Shang et al. (1996a, b), are re-examined and further investigated in this section. Thus, some improved mathematical forms of the solutions are found and the asymptotic behavior is discussed. Furthermore, a proper dimensional treatment of physical units was introduced.

3.1. Problem 1: Penny-shaped crack under uniform temperature

3.1.1. *Formulation of the problem*

A penny-shaped crack with radius a in an infinite transversely isotropic thermopiezoelectric body was considered. Both crack faces are uniformly exposed to constant temperature θ_0 differing from that of the surrounding material, see Figure 1. The complete boundary conditions are given by:

(1) thermal boundary conditions

$$\left.\begin{array}{ll} \theta = \theta_0, & 0 \leqslant \rho < a,\ z = 0 \\ \theta = 0, & \rho > a,\ z = 0 \end{array}\right\} \tag{8a}$$

and (2) mechanical and electric boundary conditions

$$\left.\begin{array}{ll} \sigma_{zz} = \sigma_{z\rho} = D_z = 0, & 0 \leqslant \rho < a,\ z = 0 \\ \sigma_{z\rho} = u_z = \varphi = 0, & \rho > a,\ z = 0 \end{array}\right\}. \tag{8b}$$

The regularity conditions at distance far away from the crack are prescribed as well.

3.1.2. *Thermopiezoelectric field*

The temperature field satisfying the above boundary value problem is

$$\theta(\rho, z) = a\theta_0 \int_0^\infty J_1(\zeta a) J_0(\zeta\rho) e^{-\zeta z/\kappa} d\zeta. \tag{9}$$

Thus, the potential function $\psi(\rho, z)$ can be written as

$$\psi(\rho, z) = a\theta_0 \int_0^\infty C(\zeta) J_1(\zeta a) J_0(\zeta\rho) e^{-\zeta z/\kappa} d\zeta. \tag{10}$$

The potential functions $\psi_1,\ \psi_2, \psi_3$ satisfying Eqs. (8b) are

$$\begin{aligned} \psi_1(\rho, z) &= \frac{\gamma_1}{a_1} \int_0^\infty D_1(\zeta) J_0(\zeta\rho) e^{-\zeta z/\gamma_1} d\zeta \\ \psi_2(\rho, z) &= \frac{\gamma_2}{a_2} \int_0^\infty D_2(\zeta) J_0(\zeta\rho) e^{-\zeta z/\gamma_2} d\zeta \\ \psi_3(\rho, z) &= -\frac{\gamma_3}{a_3} \int_0^\infty \left[D_1(\zeta) + D_2(\zeta) + \frac{a a_4 \theta_0}{\kappa} C(\zeta) J_1(\zeta a) \right] J_0(\zeta\rho) e^{-\zeta z/\gamma_3} d\zeta, \end{aligned} \tag{11}$$

where $D_1(\zeta)$ and $D_2(\zeta)$ are obtained by solving a pair of dual-integral equations as

$$\left.\begin{array}{ll} \displaystyle\int_0^\infty \zeta [\zeta D_i(\zeta) + a\alpha_i\theta_0 J_1(\zeta a)/\zeta] J_0(\zeta\rho) d\zeta = (\alpha_i - \beta_i)\theta_0, & \rho < a \\ \displaystyle\int_0^\infty [\zeta D_i(\zeta) + a\alpha_i\theta_0 J_1(\zeta a)/\zeta] J_0(\zeta\rho) d\zeta = 0, & \rho > a \end{array}\right\} \quad i = 1,\ 2 \tag{12}$$

i.e.,

$$\zeta D_i(\zeta) = aN_i\theta_0\left[\zeta^{-2}\sin(\zeta a) - a\zeta^{-1}\cos(\zeta a)\right] - a\,\alpha_i\theta_0\zeta^{-1}J_1(\zeta a) \tag{13a}$$

with

$$N_i = 2(\alpha_i - \beta_i)\big/\pi \qquad i = 1,\ 2 \tag{13b}$$

$$\alpha_1 = \frac{ma_4}{\kappa}\cdot\frac{\left(\frac{l_{22}}{a_2}-\frac{l_{23}}{a_3}\right)\left(\frac{l_{14}}{a_4}-\frac{l_{13}}{a_3}\right)-\left(\frac{l_{12}}{a_2}-\frac{l_{13}}{a_3}\right)\left(\frac{l_{24}}{a_4}-\frac{l_{23}}{a_3}\right)}{\left(\frac{l_{22}}{a_2}-\frac{l_{23}}{a_3}\right)\left(\frac{l_{11}}{a_1}-\frac{l_{13}}{a_3}\right)-\left(\frac{l_{12}}{a_2}-\frac{l_{13}}{a_3}\right)\left(\frac{l_{21}}{a_1}-\frac{l_{23}}{a_3}\right)} \tag{13c}$$

$$\alpha_2 = \frac{ma_4}{\kappa}\cdot\frac{\left(\frac{l_{21}}{a_1}-\frac{l_{23}}{a_3}\right)\left(\frac{l_{14}}{a_4}-\frac{l_{13}}{a_3}\right)-\left(\frac{l_{11}}{a_1}-\frac{l_{13}}{a_3}\right)\left(\frac{l_{24}}{a_4}-\frac{l_{23}}{a_3}\right)}{\left(\frac{l_{21}}{a_1}-\frac{l_{23}}{a_3}\right)\left(\frac{l_{12}}{a_2}-\frac{l_{13}}{a_3}\right)-\left(\frac{l_{11}}{a_1}-\frac{l_{13}}{a_3}\right)\left(\frac{l_{22}}{a_2}-\frac{l_{23}}{a_3}\right)} \tag{13d}$$

$$\beta_1 = \frac{ma_4}{\kappa}\cdot\frac{(\kappa-\gamma_3)\left(\frac{d_2}{a_2}\gamma_2-\frac{d_3}{a_3}\gamma_3\right)-(\gamma_2-\gamma_3)\left(\frac{d_4}{a_4}\kappa-\frac{d_3}{a_3}\gamma_3\right)}{(\gamma_1-\gamma_3)\left(\frac{d_2}{a_2}\gamma_2-\frac{d_3}{a_3}\gamma_3\right)-(\gamma_2-\gamma_3)\left(\frac{d_1}{a_1}\gamma_1-\frac{d_3}{a_3}\gamma_3\right)} \tag{13e}$$

$$\beta_2 = \frac{ma_4}{\kappa}\cdot\frac{(\kappa-\gamma_3)\left(\frac{d_1}{a_1}\gamma_2-\frac{d_3}{a_3}\gamma_3\right)-(\gamma_1-\gamma_3)\left(\frac{d_4}{a_4}\kappa-\frac{d_3}{a_3}\gamma_3\right)}{(\gamma_2-\gamma_3)\left(\frac{d_1}{a_1}\gamma_1-\frac{d_3}{a_3}\gamma_3\right)-(\gamma_1-\gamma_3)\left(\frac{d_2}{a_2}\gamma_2-\frac{d_3}{a_3}\gamma_3\right)}. \tag{13f}$$

The mechanical displacements, stresses, electric potential and electric displacements can thus be derived. To represent the final expressions concisely, the following notations of integrals are introduced, which were extended from the symbols defined by Sneddon (1951, 1969) and that adopted by Fan (1978) and Shang et al. (1996a, b, c), as dimensionless functions of (ρ, z)

$$\begin{aligned} S_i(m,n) &= a^{n+1}\int_0^\infty \zeta^n \sin(\zeta a)\, J_m(\zeta\rho)e^{-\zeta z/\gamma_i}d\zeta \\ I_i(m,n) &= a^{n}\int_0^\infty \zeta^{n-1} \cos(\zeta a)\, J_m(\zeta\rho)e^{-\zeta z/\gamma_i}d\zeta \\ T_i(m,n) &= a^{n+1}\int_0^\infty \zeta^n J_1(\zeta a)J_m(\zeta\rho)e^{-\zeta z/\gamma_i}d\zeta. \end{aligned} \tag{14}$$

The subscript i corresponds to the eigenvalue γ_i. One can readily see that $T_i(0,0)$ and $T_i(1,0)$ are T_i and R_i in Shang et al. (1996a, b, c), respectively. Adopting these symbols, we have

$$u_z = aN_1\theta_0\left\{\frac{l_{13}}{a_3}[S_3(0,-2) - I_3(0,0)] - \frac{l_{11}}{a_1}[S_1(0,-2) - I_1(0,0)]\right\} +$$

$$N_2\theta_0\left\{\frac{l_{13}}{a_3}[S_3(0,-2)-I_3(0,0)]-\frac{l_{12}}{a_2}[S_2(0,-2)-I_2(0,0)]\right\}+$$
$$a\theta_0\left\{\frac{l_{11}}{a_1}\alpha_1T_1(0,-1)+\frac{l_{12}}{a_2}\alpha_2T_2(0,-1)-\frac{l_{13}}{a_3}\left(\alpha_1+\alpha_2-\frac{ma_4}{\kappa}\right)T_3(0,-1)+\right.$$
$$\left.\frac{ml_{14}}{\kappa}T_4(0,-1)\right\} \tag{15}$$

$$\begin{aligned}\sigma_{zz} &= N_1\theta_0\{\gamma_1[S_1(0,-1)-I_1(0,1)]-\gamma_3[S_3(0,-1)-I_3(0,1)]\}+\\ &\quad N_2\theta_0\{\gamma_2[S_2(0,-1)-I_2(0,1)]-\gamma_3[S_3(0,-1)-I_3(0,1)]\}-\\ &\quad \theta_0\left\{\gamma_1\alpha_1T_1(0,0)+\gamma_2\alpha_2T_2(0,0)-\gamma_3\left(\alpha_1+\alpha_2-\frac{ma_4}{\kappa}\right)T_3(0,0)+\right.\\ &\quad \left.a_4mT_4(0,0)\right\}\end{aligned} \tag{16}$$

$$\begin{aligned}\varphi &= aN_1\theta_0\left\{\frac{l_{23}}{a_3}[S_3(0,-2)-I_3(0,0)]-\frac{l_{21}}{a_1}[S_1(0,-2)-I_1(0,0)]\right\}+\\ &\quad aN_2\theta_0\left\{\frac{l_{23}}{a_3}[S_3(0,-2)-I_3(0,0)]-\frac{l_{22}}{a_2}[S_2(0,-2)-I_2(0,0)]\right\}+\\ &\quad a\theta_0\left\{\frac{l_{21}}{a_1}\alpha_1T_1(0,-1)+\frac{l_{22}}{a_2}\alpha_2T_2(0,-1)-\frac{l_{23}}{a_3}\left(\alpha_1+\alpha_2-\frac{ma_4}{\kappa}\right)T_3(0,-1)+\right.\\ &\quad \left.\frac{ml_{24}}{\kappa}T_4(0,-1)\right\}\end{aligned} \tag{17}$$

$$\begin{aligned}D_z &= N_1\theta_0\left\{\frac{d_1\gamma_1}{a_1}[S_1(0,-1)-I_1(0,1)]-\frac{d_3\gamma_3}{a_3}[S_3(0,-1)-I_3(0,1)]\right\}+\\ &\quad N_2\theta_0\left\{\frac{d_2\gamma_2}{a_2}[S_2(0,-1)-I_2(0,1)]-\frac{d_3\gamma_3}{a_3}[S_3(0,-1)-I_3(0,1)]\right\}-\\ &\quad \theta_0\left\{\frac{d_1\gamma_1}{a_1}\alpha_1T_1(0,0)+\frac{d_2\gamma_2}{a_2}\alpha_2T_2(0,0)-\frac{d_3\gamma_3}{a_3}\left(\alpha_1+\alpha_2-\frac{ma_4}{\kappa}\right)T_3(0,0)-\right.\\ &\quad \left.d_4mT_4(0,0)\right\}.\end{aligned} \tag{18}$$

3.1.3. *Asymptotic behavior at the crack tip*

Due to the importance of crack tip behavior, a local polar coordinate system (r, ω) along the crack front in the meridional plane is introduced, Figure 2. This local coordinate system is needed to find the asymptotic solution of a crack in thermopiezoelectric materials as limiting case $r \to 0$. This technique was adopted from Sneddon (1951) for the cases of elastic crack analysis. When applying to crack problems in thermopiezoelectric materials, care should be taken on interpreting the correlation between those geometric definitions and the material eigenvalues, which will be illustrated below.

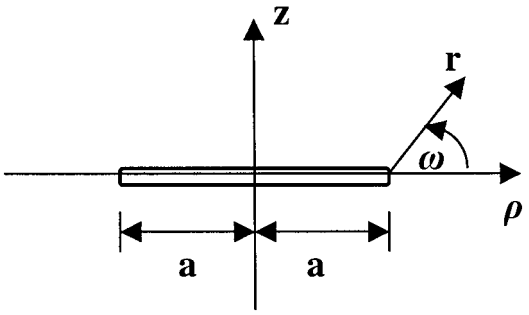

Figure 2. Local polar coordinates (r, ω) at the crack tip.

To consider asymptotic behavior at the crack tip, the geometric quantities $r_i, \omega_i, z_i,\ i = 1, 2, 3$ are introduced corresponding to the eigenvalues γ_i of the thermopiezoelectric material as

$$\left.\begin{array}{l} z_i = z/\gamma_i = r_i \sin\omega_i \\ r_i \cos\omega_i = r\cos\omega \end{array}\right\} \quad i = 1, 2, 3. \tag{19}$$

Noting that $\rho = 1 + r\cos\omega,\ \ z = r\sin\omega$ from Figure 2, we have

$$\left.\begin{array}{l} \omega_i = \tan^{-1}\left(\dfrac{\tan\omega}{\gamma_i}\right) \\ r_i = r\dfrac{\cos\omega}{\cos\omega_i} \end{array}\right\} \quad i = 1, 2, 3. \tag{20}$$

The quantities r_i, ω_i are useful for deriving the integrals appeared in Eqs. (15-18), but they should not be understood as another local coordinates despite of the above relations. When only the principal terms of Eqs. (15–18) near the crack tip are considered, we have

$$S_i(0,-2) - I_i(0,0) = \sqrt{\frac{2r_i}{a}}\sin\frac{\omega_i}{2}, \qquad S_i(0,-1) - I_i(0,1) = -\sqrt{\frac{a}{2r_i}}\cos\frac{\omega_i}{2}. \tag{21}$$

In general, the integrals $T_i(m, n)$ cannot be expressed with elementary functions, therefore, only the special cases of crack plane is considered. These cases are useful for assessing the asymptotic behavior at the crack tip. When $z = 0$ and $\rho > a$, we have

$$T_i(0,0) = 0, \qquad T_i(0,-1) = \left(\frac{a}{2r_i}\right)\cdot {}_2F_1\left(\frac{1}{2}, \frac{1}{2}; 2; \frac{a^2}{r_i^2}\right), \qquad T_i(1,-1) = \frac{a}{2r_i}, \tag{22}$$

where ${}_2F_1(a, b; c; z)$ is hypergeometric function (see Abramowitz and Stegun, 1972; Gradstejn and Ryzik, 1980). It's found that the terms involving $T_i(0, 0)$ have no contribution on stress-intensity factors. By expanding the integral $T_i(0, -1)$ into series, we also found that no terms involving $\sqrt{2r_i}$ existed. Based upon these findings, Eqs. (15–18) can be rewritten as

$$\begin{aligned} u_z \;=\; & \sqrt{a}N_1\theta_0\left(\frac{l_{13}}{a_3}\sqrt{2r_3}\sin\frac{\omega_3}{2} - \frac{l_{11}}{a_1}\sqrt{2r_1}\sin\frac{\omega_1}{2}\right) \;+ \\ & \sqrt{a}N_2\theta_0\left(\frac{l_{13}}{a_3}\sqrt{2r_3}\sin\frac{\omega_3}{2} - \frac{l_{12}}{a_2}\sqrt{2r_2}\sin\frac{\omega_2}{2}\right) \end{aligned} \tag{23}$$

$$\sigma_{zz} = \sqrt{a}N_1\theta_0\left(\frac{\gamma_3}{\sqrt{2r_3}}\cos\frac{\omega_3}{2} - \frac{\gamma_1}{\sqrt{2r_1}}\cos\frac{\omega_1}{2}\right) + \sqrt{a}N_2\theta_0\left(\frac{\gamma_3}{\sqrt{2r_3}}\cos\frac{\omega_3}{2} - \frac{\gamma_2}{\sqrt{2r_2}}\cos\frac{\omega_2}{2}\right) \tag{24}$$

$$\varphi = \sqrt{a}N_1\theta_0\left(\frac{l_{23}}{a_3}\sqrt{2r_3}\sin\frac{\omega_3}{2} - \frac{l_{21}}{a_1}\sqrt{2r_1}\sin\frac{\omega_1}{2}\right) + \sqrt{a}N_2\theta_0\left(\frac{l_{23}}{a_3}\sqrt{2r_3}\sin\frac{\omega_3}{2} - \frac{l_{22}}{a_2}\sqrt{2r_2}\sin\frac{\omega_2}{2}\right) \tag{25}$$

$$D_z = \sqrt{a}N_1\theta_0\left(\frac{d_3\gamma_3}{a_3}\frac{1}{\sqrt{2r_3}}\cos\frac{\omega_3}{2} - \frac{d_1\gamma_1}{a_1}\frac{1}{\sqrt{2r_1}}\cos\frac{\omega_1}{2}\right) + \sqrt{a}N_2\theta_0\left(\frac{d_3\gamma_3}{a_3}\frac{1}{\sqrt{2r_3}}\cos\frac{\omega_3}{2} - \frac{d_2\gamma_2}{a_2}\frac{1}{\sqrt{2r_2}}\cos\frac{\omega_2}{2}\right) \tag{26}$$

3.1.4. *Stress-intensity factors*

Using the definitions of stress- and electric displacement-intensity factors,

$$\begin{aligned} K_I &= \lim_{r\to 0}\sqrt{2\pi\, r}\,\sigma_{zz}(r,\omega=0) \\ K_{IV} &= \lim_{r\to 0}\sqrt{2\pi\, r}\,D_z(r,\omega=0) \end{aligned} \tag{27}$$

and noting that when $z = 0$, i.e., $\omega = 0$ or π, according to Eq. (20) follows $\omega_i = 0$ or π and $r_i = r,\ i = 1,\ 2,\ 3$, we have

$$\begin{aligned} K_I &= N_1\sqrt{\pi a}\theta_0(\gamma_3-\gamma_1) + N_2\sqrt{\pi a}\theta_0(\gamma_3-\gamma_2) \\ K_{IV} &= N_1\sqrt{\pi a}\theta_0\left(\frac{d_3}{a_3}\gamma_3 - \frac{d_1}{a_1}\gamma_1\right) + N_2\sqrt{\pi a}\theta_0\left(\frac{d_3}{a_3}\gamma_3 - \frac{d_2}{a_2}\gamma_2\right) \end{aligned} \tag{28}$$

The other stress-intensity factors vanish in this case.

From Eqs. (23–26) and relation (20), the asymptotic singular behavior at the crack tip could be discussed. It's found that the angular distributions of stress and electric displacement possess some complicated forms, which depends largely upon material constants. The typical simple forms of linear elastic crack solutions are no longer valid for thermopiezoelectric cases. On the contrary, their actual distributions could only be determined numerically for specific materials.

Considering the special case at the crack plane, i.e. when $z = 0$, we have

$$\begin{aligned} \sigma_{zz}(r,\omega=0) &= \sqrt{\frac{a}{2r}}\,\{N_1\theta_0(\gamma_3-\gamma_1) + N_2\theta_0(\gamma_3-\gamma_2)\} \\ D_z(r,\omega=0) &= \sqrt{\frac{a}{2r}}\left\{N_1\theta_0(\frac{d_3}{a_3}\gamma_3 - \frac{d_1}{a_1}\gamma_1) + N_2\theta_0(\frac{d_3}{a_3}\gamma_3 - \frac{d_2}{a_2}\gamma_2)\right\} \end{aligned} \tag{29}$$

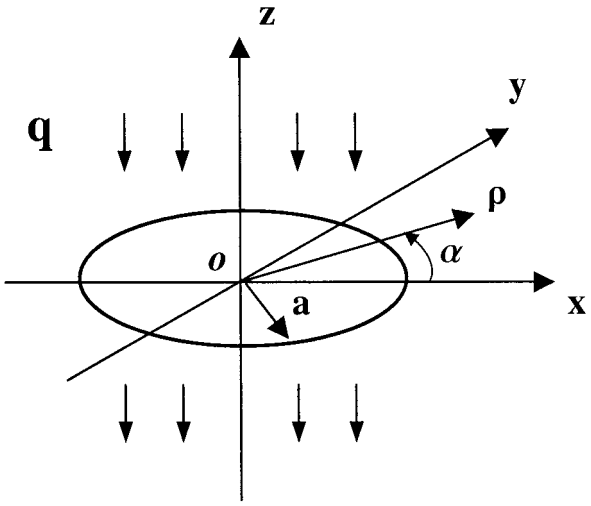

Figure 3. Penny-shaped crack under perpendicular heat flow.

and

$$\begin{aligned}
\Delta u_z &= u_z(r, \omega = \pi) - u_z(r, \omega = -\pi) \\
&= \sqrt{8ra}\left\{N_1\theta_0\left(\frac{l_{13}}{a_3} - \frac{l_{11}}{a_1}\right) + N_2\theta_0\left(\frac{l_{13}}{a_3} - \frac{l_{12}}{a_2}\right)\right\} \\
\Delta\varphi &= \varphi(r, \omega = \pi) - \varphi(r, \omega = -\pi) \\
&= \sqrt{8ra}\left\{N_1\theta_0\left(\frac{l_{23}}{a_3} - \frac{l_{21}}{a_1}\right) + N_2\theta_0\left(\frac{l_{23}}{a_3} - \frac{l_{22}}{a_2}\right)\right\}
\end{aligned} \tag{30}$$

According to Pak (1992) and Kuna (1998), there exist relations between stress-intensity factors and the opening displacement and electric potential, i.e. Eq. (30) at the crack face, as

$$\begin{Bmatrix} \Delta u_z \\ \Delta u_x \\ \Delta u_y \\ \Delta\varphi \end{Bmatrix} = \sqrt{\frac{8r}{\pi}}\,[\mathbf{Y}(c, e, \in)] \begin{Bmatrix} K_I \\ K_{II} \\ K_{III} \\ K_{IV} \end{Bmatrix} \tag{31}$$

where [**Y**] is the generalized Irwin matrix. This relation is valuable for determining stress-intensity factors as well as electromechanical energy release rate G. However, from Eqs. (28–30), the Irwin matrix for this case could not be found explicitly. This might be due to the potential function method, although other solution methods did not succeed as well.

3.2. Problem 2: Penny-shaped crack under uniform heat flow

3.2.1. *Formulation of the problem*

Consider a penny-shaped crack with radius of unit length located in the $z = 0$ plane, Figure 3. The faces of the crack are thermally insulated. There is a uniform steady flow of heat, q_0, in an infinite thermopiezoelectric medium in the direction of the negative z-axis. The original temperature field is $\theta_0 = q \cdot z$, where q is a positive constant. Noticing the anti-symmetry of this problem, the disturbing temperature field due to the crack is an odd function of z,

$$\theta(\rho, -z) = -\theta(\rho, z).$$

Accordingly, the corresponding boundary conditions are

$$\left.\begin{aligned} &\frac{\partial\theta}{\partial z} = -q, \quad 0 \leqslant \rho < a,\ z = 0 \\ &\theta = 0, \qquad\qquad \rho > a,\ z = 0 \end{aligned}\right\} \tag{32}$$

$$\left.\begin{aligned} &\sigma_{zz} = \sigma_{z\rho} = D_z = 0, \quad 0 \leqslant \rho < a,\ z = 0 \\ &\sigma_{zz} = u_\rho = D_z = 0, \qquad\quad \rho > a,\ z = 0 \end{aligned}\right\} \tag{33}$$

3.2.2. *Thermopiezoelectric field*
The temperature field satisfying the relation (32) is, when $z \geqslant 0$,

$$\theta(\rho, z) = \frac{2\kappa q}{\pi}\int_0^\infty \left[\zeta^{-2}\sin(\zeta a) - a\zeta^{-1}\cos(\zeta a)\right] J_0(\zeta\rho)\, e^{-\zeta z/\kappa} d\zeta. \tag{34}$$

To fulfill the boundary conditions, the piezoelectric potential functions are chosen as

$$\begin{aligned} \psi(\rho, z) &= \frac{2\kappa q}{\pi}\int_0^\infty \left[\zeta^{-2}\sin(\zeta a) - a\zeta^{-1}\cos(\zeta a)\right] C(\zeta)\, J_0(\zeta\rho)\, e^{-\zeta z/\kappa} d\zeta \\ \psi_1(\rho, z) &= \gamma_1^2\int_0^\infty G_1(\zeta) J_0(\zeta\rho) e^{-\zeta z/\gamma_1} d\zeta \\ \psi_2(\rho, z) &= \gamma_2^2\int_0^\infty [-n_1 G_1(\zeta) + m_1 A(\zeta)\zeta^{-2}] J_0(\zeta\rho) e^{-\zeta z/\gamma_2} d\zeta \\ \psi_3(\rho, z) &= \gamma_3^2\int_0^\infty [-n_2 G_1(\zeta) + m_2 A(\zeta)\zeta^{-2}] J_0(\zeta\rho) e^{-\zeta z/\gamma_3} d\zeta, \end{aligned} \tag{35a}$$

where

$$\begin{aligned} n_1 &= \left(\frac{\gamma_1}{\gamma_2}\right)^2 \frac{a_1 d_3 - a_3 d_1}{a_2 d_3 - a_3 d_2} \qquad n_2 = \left(\frac{\gamma_1}{\gamma_3}\right)^2 \frac{a_1 d_2 - a_2 d_1}{a_3 d_2 - a_2 d_3} \\ m_1 &= \frac{m}{\gamma_2^2}\cdot\frac{a_4 d_3 + a_3 d_4}{a_2 d_3 - a_3 d_2} \qquad m_2 = \frac{m}{\gamma_3^2}\cdot\frac{a_4 d_2 + a_2 d_4}{a_3 d_2 - a_2 d_3} \\ A(\zeta) &= \frac{2\kappa q}{\pi}\left[\zeta^{-2}\sin(\zeta a) - a\zeta^{-1}\cos(\zeta a)\right]. \end{aligned} \tag{35b}$$

The unknown $G_1(\zeta)$ is the solution of a pair of dual-integral equations as

$$\left.\begin{aligned} &\int_0^\infty \zeta[\zeta G_1(\zeta) + \eta_1 A(\zeta)/\zeta] J_1(\zeta\rho) d\zeta = (\eta_1 - \eta_2)\kappa q\rho/2, \quad \rho < a \\ &\int_0^\infty [\zeta G_1(\zeta) + \eta_1 A(\zeta)/\zeta] J_1(\zeta\rho) d\zeta = 0, \qquad\qquad \rho > a \end{aligned}\right\} \tag{36}$$

i.e.,

$$\zeta^2 G_1(\zeta) = M_1\left[\zeta^{-2}\sin(\zeta a) - a\zeta^{-1}\cos(\zeta a)\right] - M_2 a^2\sin(\zeta a), \tag{37a}$$

where

$$\begin{aligned} M_1 &= -2\eta_2\kappa q/\pi, & M_2 &= 2(\eta_1-\eta_2)\kappa q/3\pi \\ \eta_1 &= \frac{a_2m_1\gamma_2+a_3m_2\gamma_3+a_4m/\kappa}{a_1\gamma_1-a_2n_1\gamma_2-a_3n_2\gamma_3} & \eta_2 &= \frac{m_1\gamma_2^2+m_2\gamma_3^2+m}{\gamma_1^2-n_1\gamma_2^2-n_2\gamma_3^2}. \end{aligned} \tag{37b}$$

Hence, we have

$$\begin{aligned} u_\rho &= -\gamma_1^2a^2\{M_1[S_1(1,-3)-I_1(1,-1)]-M_2S_1(1,-1)\} \\ &\quad+\gamma_2^2n_1a^2\{M_1[S_2(1,-3)-I_2(1,-1)]-M_2S_2(1,-1)\} \\ &\quad+\gamma_3^2n_2a^2\{M_1[S_3(1,-3)-I_3(1,-1)]-M_2S_3(1,-1)\} \\ &\quad-\frac{2\kappa q}{\pi}a^2\{\gamma_2^2m_1[S_2(1,-3)-I_2(1,-1)] \\ &\quad+\gamma_3^2m_2[S_3(1,-3)-I_3(1,-1)]+m[S_4(1,-3)-I_4(1,-1)]\} \end{aligned} \tag{38}$$

$$\begin{aligned} \sigma_{z\rho} &= M_1a\{a_1\gamma_1[S_1(1,-2)-I_1(1,0)]-a_2\gamma_2n_1[S_2(1,-2)-I_2(1,0)] \\ &\quad-a_3\gamma_3n_2[S_3(1,-2)-I_3(1,0)]\}-M_2a\{a_1\gamma_1S_1(1,0) \\ &\quad-a_2\gamma_2n_1S_2(1,0)-a_3\gamma_3n_2S_3(1,0)\}+\frac{2\kappa q}{\pi}a\{a_2\gamma_2m_1[S_2(1,-2)-I_2(1,0)] \\ &\quad+a_3\gamma_3m_2[S_3(1,-2)-I_3(1,0)]+(a_4m/\kappa)[S_4(1,-2)-I_4(1,0)]\} \end{aligned} \tag{39}$$

To analyze the asymptotic behavior at the crack tip, the local polar coordinate system, Figure 2, is taken again for this crack problem. Referring to the integral formulae in Sneddon (1951, 1969) and Shang et al. (1996b, c) and using

$$S_i(1,-3)-I_i(1,-1)=\frac{\rho}{3a}+\frac{\pi}{6}+\frac{z_i}{3a}I_i(1,0)-\frac{\rho^2}{3a^2}S_i(1,-1)-\frac{z_i}{a}S_i(1,-2)$$

yield

$$S_i(1,-3)-I_i(1,-1)=\frac{1}{3}\sqrt{\frac{2r_i}{a}}\sin\frac{\omega_i}{2},\quad S_i(1,-1)=-\sqrt{\frac{2r_i}{a}}\sin\frac{\omega_i}{2},$$
$$S_i(1,0)=\sqrt{\frac{a}{2r_i}}\cos\frac{\omega_i}{2}$$

$$\begin{aligned} S_i(1,-2)-I_i(1,0) &= -\frac{1}{2}\sqrt{\frac{2r_i}{a}}\cos\frac{\omega_i}{2} \\ &\quad+\frac{1}{2}\tan^{-1}\left\{\left(1+\sqrt{\frac{2r_i}{a}}\sin\frac{\omega_i}{2}\right)\Big/\left(\sqrt{\frac{2r_i}{a}}\cos\frac{\omega_i}{2}\right)\right\} \end{aligned}$$

Considering only the principal values of the integrals, the displacements and stresses are

$$\begin{aligned} u_\rho &= a\sqrt{a}(M_1/3+M_2)\left[-\gamma_1^2\sqrt{2r_1}\sin\frac{\omega_1}{2}+\gamma_2^2n_1\sqrt{2r_2}\sin\frac{\omega_2}{2}+\gamma_3^2n_2\sqrt{2r_3}\sin\frac{\omega_3}{2}\right] \\ &\quad-a\sqrt{a}\frac{2\kappa q}{3\pi}\left(\gamma_2^2m_1\sqrt{2r_2}\sin\frac{\omega_2}{2}+\gamma_3^2m_2\sqrt{2r_3}\sin\frac{\omega_3}{2}+m\sqrt{2r_4}\sin\frac{\omega_4}{2}\right) \end{aligned} \tag{40}$$

$$\sigma_{z\rho} = a\sqrt{a}M_2\left(-a_1\gamma_1\frac{1}{\sqrt{2r_1}}\cos\frac{\omega_1}{2} + a_2\gamma_2 n_1\frac{1}{\sqrt{2r_2}}\cos\frac{\omega_2}{2} + a_3\gamma_3 n_2\frac{1}{\sqrt{2r_3}}\cos\frac{\omega_3}{2}\right) \quad (41)$$

3.2.3. *Stress-intensity factors*
The mode II stress-intensity factor can be extracted straightforwardly

$$K_{II} = \lim_{r\to 0}\sqrt{2\pi r}\sigma_{z\rho}(r, \omega = 0) = M_2 a\sqrt{\pi a}(-a_1\gamma_1 + a_2\gamma_2 n_1 + a_3\gamma_3 n_2). \quad (42)$$

Once again, it is observed that the angular distribution of shear stress is rather complicated and related to the specific materials. This is in agreement with the conclusion obtained in the first crack analysis.

4. Finite element verifications

To examine above analytical solutions, numerical analyses of these thermally loaded crack problems are required. As illustrated in Kuna (1998), Shang et al. (2001a, b), various finite element techniques were developed for such analyses of thermopiezoelectric materials, which have been proved to be capable to take into account the influence of thermal effects on thermopiezoelectric behavior. These techniques, including CTE (singular crack-tip elements), RSE (regular standard elements), MCCI (modified crack closure integral) with three options RSI-1, -2, -3 and a procedure TPESAP (thermopiezoelectric static analysis procedure), will be exploited to analyze the above crack problems.

4.1. Problem 1

This uniform temperature covered penny-shaped crack embedded in an infinite thermopiezoelectric body is analyzed by following the procedure TPESAP. The finite element model was meshed with ABAQUS 20-node brick piezoelectric elements C3D20E. The discretized domain is ten times the crack radius to simulate the infinite body, see Figure 4. More details on FEM model was presented in Shang et al. (2001a).

In our computations, the following materials parameters are assumed

$$c_{11} = 126.0,\quad c_{12} = 55.0,\quad c_{13} = 53.0,\quad c_{33} = 117.0,\quad c_{44} = 35.3\,\text{GPa}$$
$$e_{31} = -6.5,\quad e_{33} = 23.3,\quad e_{15} = 17.0\,\text{C/m}^2,\quad \in_{11}= 1.51\times 10^{-8},$$
$$\in_{33}= 1.30\times 10^{-8}\text{C}^2/\text{Nm}^2, c_T = 62.244\,\text{GPa},\quad \kappa_{11} = 50,\quad \kappa_{33} = 75\text{W}/\text{Km},$$
$$\kappa^2 = \kappa_{33}/\kappa_{11} = 1.5,\quad \lambda_{11} = 1.97382\times 10^6,\quad \lambda_{33} = 1.4165\times 10^6\text{N}/\text{Km}^2,$$
$$p_3 = -5.4831\times 10^{-6}\text{C}/\text{Km}^2$$

Elastic, dielectric and piezoelectric constants of PZT-5H are used for verification purposes. Thermal properties, including heat conduction coefficients, stress temperature coefficients, and pyroelectric constants, are selected arbitrarily. Numerical results and analytical solutions are presented for the case of uniform temperature $\theta_0 = -100^o\text{C}$ of the crack faces.

According to the procedure TPESAP, heat transfer analysis is performed firstly. The results of calculated temperature field are sufficiently close to the analytical expression in Eq. (9) with relative errors less than 0.5%. The normalized stress intensity factors $g_I = K_I/(-\lambda_{33}\theta_0\sqrt{\pi a})$ and $g_{IV} = K_{IV}/(p_3\theta_0\sqrt{\pi a})$, and the normalized energy release rate G/G_0 with $G_0 =$

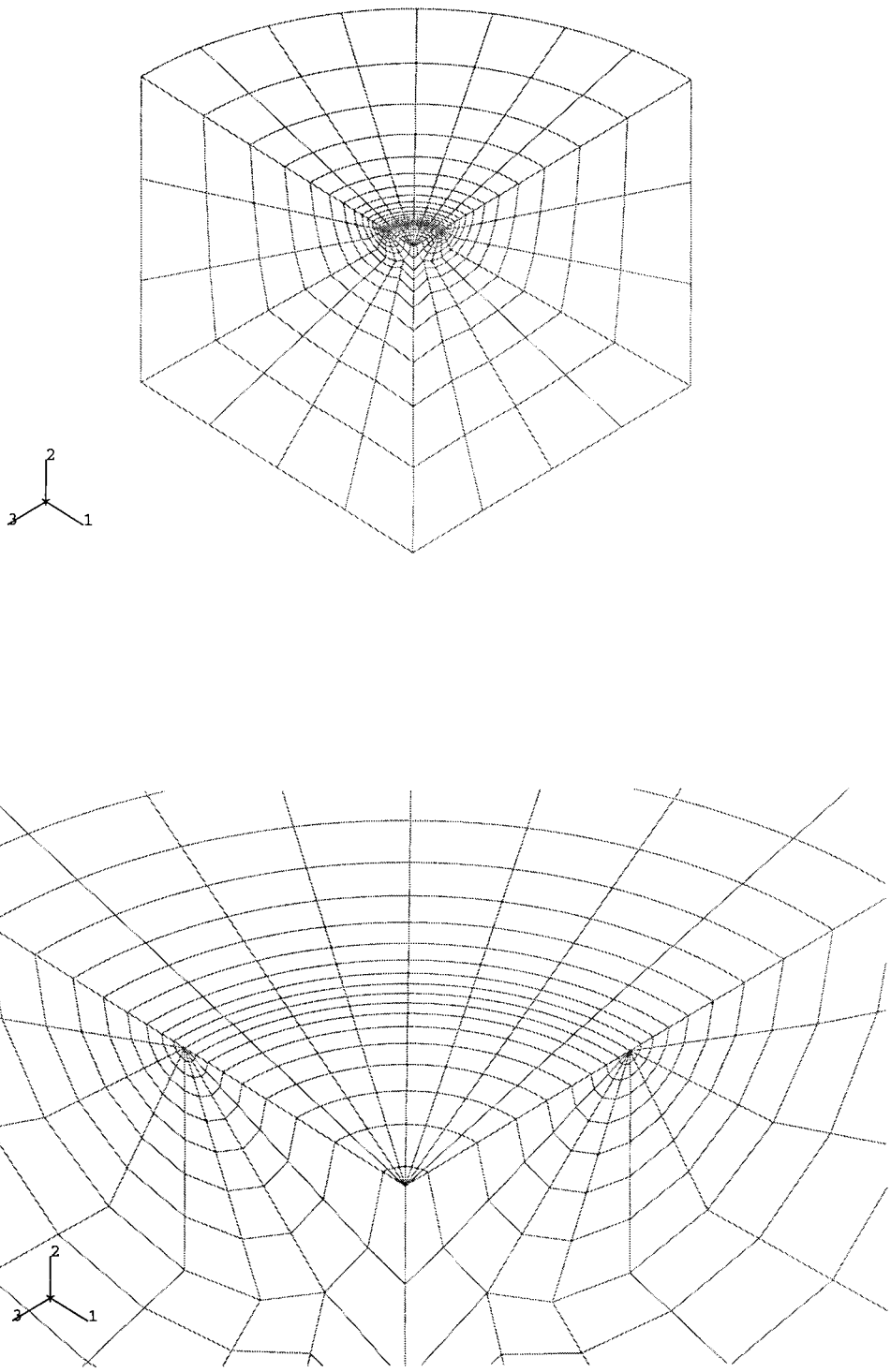

Figure 4. Finite element model of the penny-shaped crack.

Table 1. The SIFs and G results from FEM and the exact solution of problem 1.

	g_I	g_{IV}	G/G_0
Exact solution	0.199	10.830	2.394E-2
CTE direct extraction, error (%)	+0.82	−4.83	+1.2
CTE displacement extrapolation, error (%)	+2.65	−5.82	+0.1
RSE displacement extrapolation, error (%)	−1.16	−7.89	−2.8
MCCI with RSI-1, error (%)			+10.2
MCCI with RSI-2, error (%)			−17.8
MCCI with RSI-3, error (%)			−24.8
MCCI averaged, error (%)			−17.8

$(\lambda_{33}^2\theta_0^2\pi a)/c_T$ are listed in Table 1. The SIFs were derived from exact solution as well as finite element calculations. The finite element techniques involved are CTE direct extraction, CTE displacement extrapolation, and RSE displacement extrapolation. Noting that the G values for the case of exact solution are calculated by using the relation derived in Kuna (1998) with input of the exact SIFs.

From Table 1, one can see that the analytical solutions of SIFs are rather close to numerical predictions using different finite element techniques. Therefore, one conclusion is readily obtained that the analytical solution derived in Shang et al. (1996b) has been verified by the numerical results and is correct.

Comparisons of the calculated G results conclude that the CTE technique gives a better prediction of the energy release rate than the MCCI technique. The rather big errors of the G-estimations with MCCI technique are observed. The results with the option RSI-2 is also unacceptable, although it has been proved to be the best option for MCCI analyses of three-dimensional cracks. The reason might be that the finite element model follows only approximately the temperature jump across the crack front, while this temperature jump could make a substantial contribution to the energy release rate.

4.2. Problem 2

The penny-shaped crack subjected to constant heat flow $q_0 = 10K/m$ is analyzed numerically. According to Fourier's law, the heat flux s normal to the crack face is given by

$$s = -\kappa_{33}\partial\theta/\partial z = \kappa_{33}q_0.$$

Because the upper part of FEM model was considered, the calculated temperature field is described by the following expression

$$\theta(\rho, z) = -\theta(\rho, -z) = -\frac{2\kappa q_0}{\pi}\int_0^\infty \left[\zeta^{-2}\sin(\zeta a) - a\zeta^{-1}\cos(\zeta a)\right] J_0(\zeta\rho)e^{-\zeta z/\kappa}d\zeta.$$

This has been achieved numerically with relative errors less than 0.5%. The normalized SIFs $g_{II} = K_{II}/(2\kappa q_0\lambda_{33}a\sqrt{\pi a}/\pi)$and normalized G/G_0 are summarized in Table 2.
From these comparisons, we can find that the analytical expressions of SIFs obtained in Shang et al. (1996a) predict closely that of finite element analyses. Thus, the analytical solution of problem 2 has also been verified numerically.

Table 2. The SIFs and G results from FEM and the exact solutions of problem 2.

	g_{II}	G/G_0
Exact solution	0.170	9.629E-5
CTE direct extraction, error (%)	+4.0	+8.2
CTE displacement extrapolation, error (%)	−0.2	−0.4
RSE displacement extrapolation, error (%)	−3.6	−7.1
MCCI with RSI-1, error (%)		+26.2
MCCI with RSI-2, error (%)		−4.6
MCCI with RSI-3, error (%)		−11.6
MCCI average, error (%)		−7.9

The calculated results of G suggest that both the CTE and the RSI-2 techniques are able to give a good approximation of the energy release rate.

5. Conclusions

In this work, two analytical solutions of thermally loaded penny-shaped cracks in thermopiezoelectric materials are re-examined and further investigated. The analytical expressions of stress-intensity factors are verified numerically by different finite element techniques. It's also found that the angular distributions of stresses and electric displacements near the crack tip are rather complicated, which are related to elastic, piezoelectric, and dielectric constants of materials and could only be determined numerically for specific thermopiezoelectric materials.

On the other hand, the finite element techniques developed in Kuna (1998), Shang et al. (2001a, b) are tested for these crack problems. The conclusion is that the CTE technique gives a better prediction of stress-intensity factors and electromechanical energy release rate, and the MCCI technique with the option RSI-2 might be suitable for determining energy release rate with fine regular finite element mesh near the crack tip.

It should also be emphasized here that these finite element techniques have the capability to deal with more general crack configurations, e.g., elliptical crack problems, in thermopiezoelectric materials. These efforts are under investigation.

Acknowledgements

One author (F.S.) gratefully acknowledges the support provided by the Alexander von Humboldt Foundation of Germany. He also thanks Mr F. Rabold for his help on numerical analysis and Mr M. Abendroth for providing the FEM model.

References

Abramowitz, M. and Stegun, I.A. (1972). *Handbook of Mathematical Functions with Formulas, Graphs, and Mathematical Tables*. Dover, New York.

Chen, W.Q. and Shioya, T. (1999). Fundamental solution for a penny-shaped crack in a piezoelectric medium. *Journal of the Mechanics and Physics of Solids* **47**, 1459–1475.

Fan, T.Y. (1978). *Fundamentals of Fracture Mechanics*. Jiangsu Science and Technology Press, Nanjing, P. R. China.

Gradstejn, I.S. and Ryzik, I.M. (1980). *Table of Integrals, Series, and Products*. Academic Press, New York.

Kuna, M. (1998). Finite element analyses of crack problems in piezoelectric structures. *Computational Materials Science* **13**, 67–80.

Pak, Y.E. (1992). Linear electro-elastic fracture mechanics of piezoelectric materials. *International Journal of Fracture* **54**, 79–100.

Qin, Q.H. (1998). A new solution for thermopiezoelectric solid with an insulated elliptical hole. *Acta Mechanica Sinica* **14**, 157–170.

Shang, F., Kuna, M. and Abendroth, M. (2001a). Finite element analyses of three-dimensional crack problems in piezoelectric structures. submitted to *Engineering Fracture Mechanics*.

Shang, F., Kuna, M. and Scherzer, M. (2001b). Development of finite element techniques for three-dimensional analysis of thermopiezoelectric materials. Accepted by *EUROMECH Colloquium 429: Computational and Experimental Mechanics of Advanced Materials*, 19–20 September, Vienna, Austria.

Shang, F., Wang, Z.K. and Li, Z.H. (1996a). A general solution based on potential functions for three-dimensional axisymmetric problems of thermopiezoelectric solids. *Journal of Xi'an Jiaotong University* **30**, 99–110.

Shang, F., Wang, Z.K. and Li, Z.H. (1996b). Thermal stresses analysis of a three-dimensional crack in a thermopiezoelectric solid. *Engineering Fracture Mechanics* **55**, 737–750.

Shang, F., Wang, Z.K. and Li, Z.H. (1996c). Exact mechanical analysis of thermo-piezoelectric materials and laminated structures with piezoelectric layers. Ph.D. Thesis, Xi'an Jiaotong University, Xi'an, P. R. China.

Sneddon, I.N. (1951). *Fourier Transform*. McGraw-Hill, New York.

Sneddon, I.N. and Lowengrub, M. (1969). *Crack Problems in the Classical Theory of Elasticity*. John Wiley and Sons, New York.

Sosa, H.A. and Pak, Y.E. (1990). Three-dimensional eigenfunction analysis of a crack in a piezoelectric material. *International Journal of Solids and Structures* **26**, 1–15.

Sosa, H.A. (1991). Plane problems in piezoelectric media with defects. *International Journal of Solids and Structures* **28**, 491–505.

Suo, Z., Kuo, C.M., Barnett, D.M. and Willis J.R. (1992). Fracture mechanics for piezoelectric ceramics. *Journal of the Mechanics and Physics of Solids* **40**, 739–765.

Wang, B. (1992). Three-dimensional analysis of a flat elliptical crack in a piezoelectric material. *International Journal of Engineering Science* **30**, 781–791.

Wang, Z.K. (1994). Penny-shaped crack in transversely isotropic piezoelectric materials. *Acta Mechanica Sinica* **10**, 49–60.

Wang, Z.K. and Huang, S.H. (1995). Stress intensification near an elliptical border. *Theoretical and Applied Fracture Mechanics* **22**, 229–237.

Yu, S.W. and Qin, Q.H. (1996). Damage analysis of thermopiezoelectric properties: Part I – crack tip singularities. *Theoretical and Applied Fracture Mechanics* **25**, 263–277.